

Dynamical Control of Quantum Josephson Junction

Nicolas Heimann

Zentrum für optische Quantentechnologien und Institut für Laserphysik,
Universität Hamburg

June 4th 2019

Outline

Introduction

- London equations

- Response of superconductor in an AC Field

- Josephson effect

Quantum Josephson junction

- Equation of motion

- Hamiltonian

- Dissipative Model

- Equilibrium response

Dynamical Control

- Parametric driving

- Thermal modes

- Effective Josephson Energy

Summary

Introduction

High temperature superconductivity

High temperature superconductivity gathered a lot of attention in condensed matter physics.

High temperature superconductivity

High temperature superconductivity gathered a lot of attention in condensed matter physics.

1987, discovery of yttrium-barium-copper-oxide (YBCO), which has $T_c \sim 90K$ (nitrogen boiling point $\sim 77K$).

High temperature superconductivity

High temperature superconductivity gathered a lot of attention in condensed matter physics.

1987, discovery of yttrium-barium-copper-oxide (YBCO), which has $T_c \sim 90K$ (nitrogen boiling point $\sim 77K$).

Common feature YBCO and similar ceramics share are copper oxide (CuO) layers.

High temperature superconductivity

High temperature superconductivity gathered a lot of attention in condensed matter physics.

1987, discovery of yttrium-barium-copper-oxide (YBCO), which has $T_c \sim 90K$ (nitrogen boiling point $\sim 77K$).

Common feature YBCO and similar ceramics share are copper oxide (CuO) layers.

The CuO layers are assumed to be the host of superconductivity.

High temperature superconductivity

High temperature superconductivity gathered a lot of attention in condensed matter physics.

1987, discovery of yttrium-barium-copper-oxide (YBCO), which has $T_c \sim 90K$ (nitrogen boiling point $\sim 77K$).

Common feature YBCO and similar ceramics share are copper oxide (CuO) layers.

The CuO layers are assumed to be the host of superconductivity.

Lawrence-Doniac model: Weakly coupled layer structure phenomenologically modeled as coupled Josephson junctions.

pump-probe experiments

Pump-probe experiments allow to gain insights into non-equilibrium states.

pump-probe experiments

Pump-probe experiments allow to gain insights into non-equilibrium states.

In 2013, Andrea Cavalleri et al. observed the phenomenon of optically enhanced coherence.

pump-probe experiments

Pump-probe experiments allow to gain insights into non-equilibrium states.

In 2013, Andrea Cavalleri et al. observed the phenomenon of optically enhanced coherence.

Parametric driving induces an enhancement of the superconductive response in bilayer systems of Josephson junctions
[HZR⁺15, OCM16, OHCM17, Hom18]

pump-probe experiments

Pump-probe experiments allow to gain insights into non-equilibrium states.

In 2013, Andrea Cavalleri et al. observed the phenomenon of optically enhanced coherence.

Parametric driving induces an enhancement of the superconductive response in bilayer systems of Josephson junctions
[HZR⁺15, OCM16, OHCM17, Hom18]

How much do quantum fluctuations play a role? Are aspects of quantization important?, i.e. a discrete energy spectrum.

London equations

The London brothers proposed the first phenomenological description of superconductivity [LLL35]. The *London equations* are

$$\vec{E} = \Lambda \frac{\partial \vec{J}}{\partial t} \quad \vec{B} = -c \Lambda \vec{\nabla} \times \vec{J} \quad \Lambda = \frac{m}{n_s q^2}. \quad (1)$$

London equations

The London brothers proposed the first phenomenological description of superconductivity [LLL35]. The *London equations* are

$$\vec{E} = \Lambda \frac{\partial \vec{J}}{\partial t} \quad \vec{B} = -c \Lambda \vec{\nabla} \times \vec{J} \quad \Lambda = \frac{m}{n_s q^2}. \quad (1)$$

- ▶ Zero DC resistance

London equations

The London brothers proposed the first phenomenological description of superconductivity [LLL35]. The *London equations* are

$$\vec{E} = \Lambda \frac{\partial \vec{J}}{\partial t} \quad \vec{B} = -c \Lambda \vec{\nabla} \times \vec{J} \quad \Lambda = \frac{m}{n_s q^2}. \quad (1)$$

- ▶ Zero DC resistance
- ▶ Meißner-Ochsenfeld effect (Type I superconductors are perfect diamagnets)

AC response of a perfect superconductor

Consider an electric field mode at angular frequency ω

$$\vec{E}(t) = \vec{E}(\omega) e^{-i\omega t}, \quad (2)$$

and the current density

$$\vec{J}(t) = \vec{J}(\omega) e^{-i\omega t}. \quad (3)$$

AC response of a perfect superconductor

Consider an electric field mode at angular frequency ω

$$\vec{E}(t) = \vec{E}(\omega) e^{-i\omega t}, \quad (2)$$

and the current density

$$\vec{J}(t) = \vec{J}(\omega) e^{-i\omega t}. \quad (3)$$

Integrating the first London equation yields (for $\omega > 0$)

$$i \frac{\vec{E}(\omega)}{\Lambda \omega} = \vec{J}(\omega). \quad (4)$$

AC response of a perfect superconductor

Consider an electric field mode at angular frequency ω

$$\vec{E}(t) = \vec{E}(\omega)e^{-i\omega t}, \quad (2)$$

and the current density

$$\vec{J}(t) = \vec{J}(\omega)e^{-i\omega t}. \quad (3)$$

Integrating the first London equation yields (for $\omega > 0$)

$$i \frac{\vec{E}(\omega)}{\Lambda\omega} = \vec{J}(\omega). \quad (4)$$

Ohm's law $\vec{J}(\omega) = \sigma(\omega)\vec{E}(\omega)$ identifies a pure imaginary conductivity

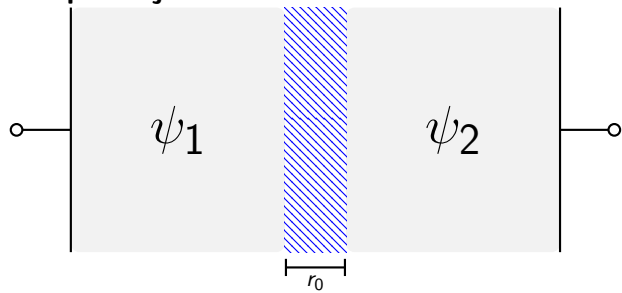
$$\sigma = i \frac{nq^2}{m\omega}. \quad (5)$$

Thus, the current response obeys a $\pi/2$ phase shift.

Tunneling junctions

How do supercurrents tunnel between two superconducting sites separated by a non-superconductive barrier?

Josephson junction



$$\begin{aligned}\psi_{1,2} &= |\psi_{1,2}| \exp(i\phi_{1,2}) \\ \phi &\equiv \phi_1 - \phi_2\end{aligned}\tag{6}$$

Josephson equations

In 1962, Brian Josephson proposed the two *Josephson equations* [Jos62]

$$\begin{aligned} I &\sim \sin \phi \\ \frac{\partial \phi}{\partial t} &\sim V. \end{aligned} \tag{7}$$

Josephson equations

In 1962, Brian Josephson proposed the two *Josephson equations* [Jos62]

$$\begin{aligned} I &\sim \sin \phi \\ \frac{\partial \phi}{\partial t} &\sim V. \end{aligned} \tag{7}$$

DC-Josephson effect: A finite junction current can flow through the barrier, even at absence of voltage.

Josephson equations

In 1962, Brian Josephson proposed the two *Josephson equations* [Jos62]

$$\begin{aligned} I &\sim \sin \phi \\ \frac{\partial \phi}{\partial t} &\sim V. \end{aligned} \tag{7}$$

DC-Josephson effect: A finite junction current can flow through the barrier, even at absence of voltage.

In 1963, Anderson and Rowell observed the DC-Josephson effect in experiment [AR63]

AC-Josephson effect

AC-Josephson effect: A stationary electric potential difference $V = \text{const}$ leads to an oscillating junction current

$$I \sim \sin(\omega t). \quad (8)$$

Quantum Josephson junction

Equation of motion

The two Josephson equations allow to evaluate $\ddot{\phi}$. An equation of motion is obtained

$$\frac{\partial^2 \phi}{\partial t^2} + \frac{2\pi}{\Phi_0} \frac{I_c}{C} \sin \phi = \frac{2\pi}{\Phi_0} \frac{I_e}{C} \quad (9)$$

I_c : critical junction current

I_e : external current

C : capacitance

Quantization

The latter equation is the Euler-Lagrange equation of the Lagrange function of a pendulum

$$L = \frac{C}{2} \left(\frac{\Phi_0}{2\pi} \right)^2 \dot{\phi}^2 + \frac{\Phi_0}{2\pi} (I_c \cos \phi + I_e \phi). \quad (10)$$

Quantization

The latter equation is the Euler-Lagrange equation of the Lagrange function of a pendulum

$$L = \frac{C}{2} \left(\frac{\Phi_0}{2\pi} \right)^2 \dot{\phi}^2 + \frac{\Phi_0}{2\pi} (I_c \cos \phi + I_e \phi). \quad (10)$$

- ▶ Canonical conjugate to the phase $\chi = \frac{\partial L}{\partial \dot{\phi}}$.

Quantization

The latter equation is the Euler-Lagrange equation of the Lagrange function of a pendulum

$$L = \frac{C}{2} \left(\frac{\Phi_0}{2\pi} \right)^2 \dot{\phi}^2 + \frac{\Phi_0}{2\pi} (I_c \cos \phi + I_e \phi). \quad (10)$$

- ▶ Canonical conjugate to the phase $\chi = \frac{\partial L}{\partial \dot{\phi}}$.
- ▶ Legendre transformation yields the Hamiltonian $H = \chi \dot{\phi} - L$.

Quantization

The latter equation is the Euler-Lagrange equation of the Lagrange function of a pendulum

$$L = \frac{C}{2} \left(\frac{\Phi_0}{2\pi} \right)^2 \dot{\phi}^2 + \frac{\Phi_0}{2\pi} (I_c \cos \phi + I_e \phi). \quad (10)$$

- ▶ Canonical conjugate to the phase $\chi = \frac{\partial L}{\partial \dot{\phi}}$.
- ▶ Legendre transformation yields the Hamiltonian $H = \chi \dot{\phi} - L$.
- ▶ **Quantization:** Impose an uncertainty between the conjugate variables $[\phi, \chi] = i\hbar$.

Hamiltonian

Quantized Josephson junction Hamiltonian

$$H = \frac{E_c}{2} \delta n^2 - J_0 \cos(\phi) + \frac{\Phi_0}{2\pi} I_e \phi. \quad (11)$$

Hamiltonian

Quantized Josephson junction Hamiltonian

$$H = \frac{E_c}{2} \delta n^2 - J_0 \cos(\phi) + \frac{\Phi_0}{2\pi} I_e \phi. \quad (11)$$

Charge operator $\delta n = -i \frac{\partial}{\partial \phi}$.

Hamiltonian

Quantized Josephson junction Hamiltonian

$$H = \frac{E_c}{2} \delta n^2 - J_0 \cos(\phi) + \frac{\Phi_0}{2\pi} I_e \phi. \quad (11)$$

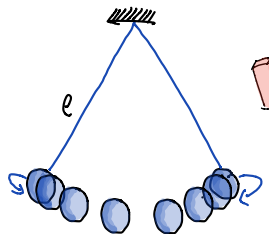
Charge operator $\delta n = -i \frac{\partial}{\partial \phi}$.

Characterizing energy scales:

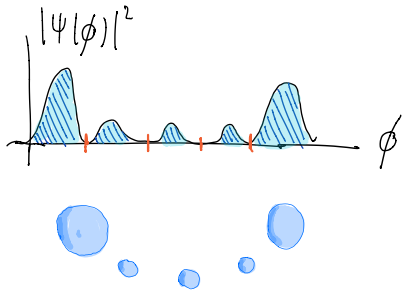
$$E_c = \left(\frac{2\pi\hbar}{\Phi_0} \right)^2 \frac{1}{C} \quad \text{charge energy} \quad (12)$$

$$J_0 = \frac{\Phi_0}{2\pi} I_c \quad \text{Josephson energy} \quad (13)$$

Classical vs. quantum pendulum



VS



$$\phi(t)$$

$$E = T + V$$

$$\omega_0 = \sqrt{g/l}$$

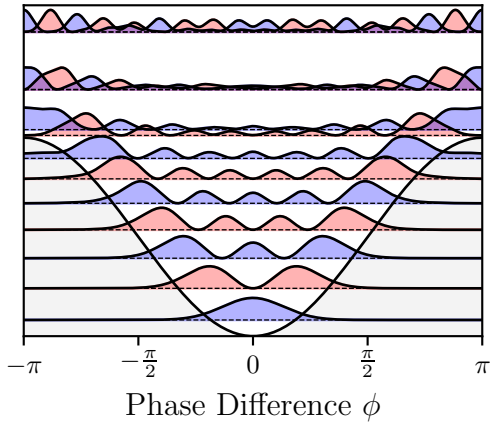
$$|\psi(\phi)|^2$$

$$H\psi = E\psi$$

$$\hbar\omega_0 = \sqrt{E_c J_0}$$

Josephson regime

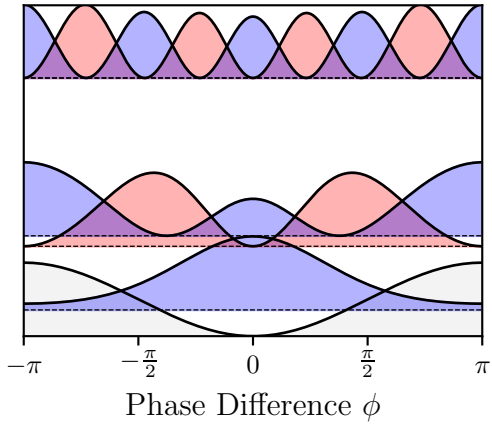
$$|\psi(\phi)|^2$$



$$\eta = \frac{E_c}{J_0} = 0.1 \quad (14)$$

Charge regime

$$|\psi(\phi)|^2$$



$$\eta = \frac{E_c}{J_0} = 1 \quad (15)$$

Dissipation

Schrödinger equation generates unitary time evolution

$$\psi(t) = U(t)\psi(0) \quad (16)$$

Dissipation

Schrödinger equation generates unitary time evolution

$$\psi(t) = U(t)\psi(0) \quad (16)$$

Timereversal

$$\underbrace{U^\dagger(t)}_{=U^{-1}(t)} U(t) = \text{Id} \quad (17)$$

Dissipation

Schrödinger equation generates unitary time evolution

$$\psi(t) = U(t)\psi(0) \quad (16)$$

Timereversal

$$\underbrace{U^\dagger(t)}_{=U^{-1}(t)} U(t) = \text{Id} \quad (17)$$

Real systems are subject to decoherence and dissipation which is not captured by the unitary evolution.

Open quantum systems

Add another system B which acts as a Reservoir of "energy" and "entropy".

$$H = H_S \otimes \text{Id}_B + \text{Id}_S \otimes H_B + \alpha V \in \mathcal{H}_S \otimes \mathcal{H}_B \quad (18)$$

Open quantum systems

Add another system B which acts as a Reservoir of "energy" and "entropy".

$$H = H_S \otimes \text{Id}_B + \text{Id}_S \otimes H_B + \alpha V \in \mathcal{H}_S \otimes \mathcal{H}_B \quad (18)$$

Under weak coupling conditions, the non-unitary dynamics of the reduced system is generated by the *Lindblad master equation*

$$\mathcal{L}\rho_S = -i[H, \rho_S] + \sum_{\alpha} \left(A_{\alpha} \rho_S A_{\alpha}^{\dagger} - \frac{1}{2} \{ A_{\alpha}^{\dagger} A_{\alpha}, \rho_S \} \right) \quad (19)$$

Open quantum systems

Add another system B which acts as a Reservoir of "energy" and "entropy".

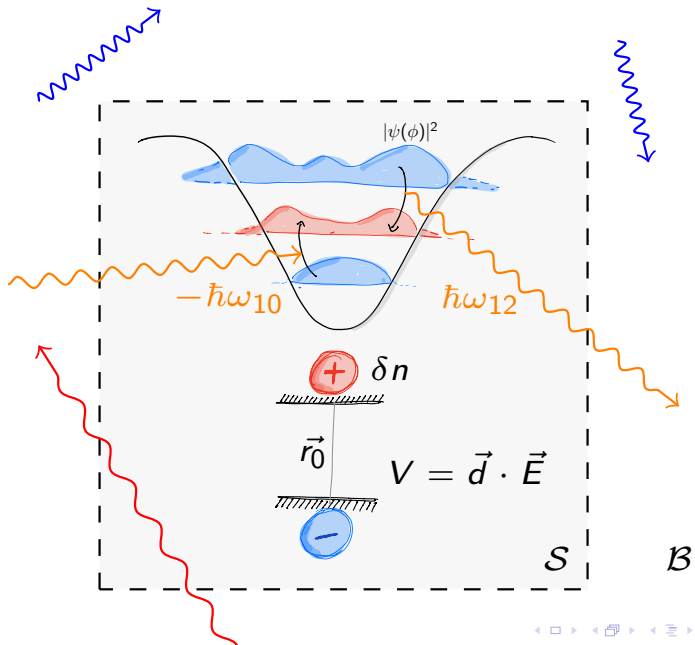
$$H = H_S \otimes \text{Id}_B + \text{Id}_S \otimes H_B + \alpha V \in \mathcal{H}_S \otimes \mathcal{H}_B \quad (18)$$

Under weak coupling conditions, the non-unitary dynamics of the reduced system is generated by the *Lindblad master equation*

$$\mathcal{L}\rho_S = -i[H, \rho_S] + \sum_{\alpha} \left(A_{\alpha} \rho_S A_{\alpha}^{\dagger} - \frac{1}{2} \{ A_{\alpha}^{\dagger} A_{\alpha}, \rho_S \} \right) \quad (19)$$

Book: Theory of open quantum systems by Heinz Breuer and Francesco Petruccione [BP02].

Dipole in the electromagnetic field

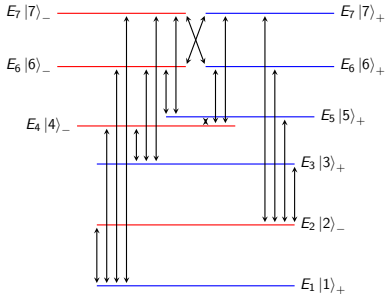


Hamiltonian

The Hamiltonian of the Josephson junction coupled by dipole interaction to the electromagnetic field is

$$\begin{aligned} H = & \left(\frac{E_c}{2} \delta n^2 - J_0 \cos(\phi) + \frac{\Phi_0}{2\pi} I \phi \right) \otimes \text{Id}_B \\ & + \text{Id}_S \otimes \sum_{k\lambda} \hbar \omega_k a_{k\lambda}^\dagger a_{k\lambda} \\ & + r_0 e_* \delta n \otimes i \sum_{k\lambda} \sqrt{\frac{2\pi\hbar\omega_k}{\epsilon_0 V}} e_{\lambda k} \left(a_k e^{ikx} - a_k^\dagger e^{-ikx} \right). \end{aligned} \tag{20}$$

B



$$\mathcal{L}\rho = -\frac{i}{\hbar} [H_S, \rho] + \sum_{\omega} \gamma(\omega) \mathcal{D} \delta n(\omega) \rho, \quad (21)$$

with the transition operators

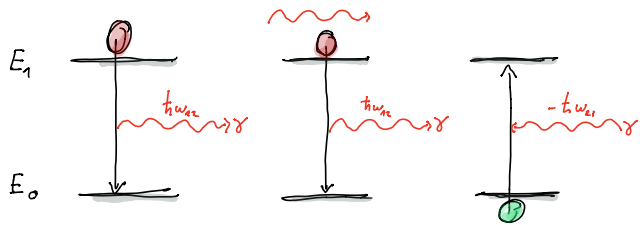
$$\delta n(\omega) = \sum_{\omega_{ab}} \delta(\omega_{ab} - \omega) \langle a | \delta n | b \rangle |a\rangle\langle b|, \quad (22)$$

and the dissipation rate

$$\gamma(\omega) = \kappa\omega^3(1 + N(\omega)). \quad (23)$$

Emission and absorption of photons

Einstein coefficients



$$\gamma \sim \omega^3$$

Spontaneous emission

$$\gamma \sim \omega^3 N(\omega)$$

Stimulated emission

$$\gamma \sim \omega^3 N(\omega)$$

Absorption

- ▶ For $\dim \mathcal{H} = 15$ circa ~ 90 Lindblad terms

- ▶ For $\dim \mathcal{H} = 15$ circa ~ 90 Lindblad terms
- ▶ Matrix products ABC of $\dim \mathcal{H} \times \dim \mathcal{H}$ matrices.

- ▶ For $\dim \mathcal{H} = 15$ circa ~ 90 Lindblad terms
- ▶ Matrix products ABC of $\dim \mathcal{H} \times \dim \mathcal{H}$ matrices.
- ▶ Optimized, GPU based implementation - qoptical ¹

¹github.com/keksnicoh/qoptical

- ▶ For $\dim \mathcal{H} = 15$ circa ~ 90 Lindblad terms
- ▶ Matrix products ABC of $\dim \mathcal{H} \times \dim \mathcal{H}$ matrices.
- ▶ Optimized, GPU based implementation - qoptical ¹
- ▶ ~ 10 arithmetic operations required per matrix element ρ_{xy} to evaluate the full dissipator.

¹github.com/keksnicoh/qoptical

Probing field

The probing field is implemented by inducing a tilt to the $J_0 \cos(\phi)$ potential

$$H(t) = \phi J_0 \delta I \cos(\omega_p t) \quad (24)$$

ω_p : Probing frequency

δI : Relative amplitude ($\delta I = 10^{-3}$)

Probing field

The probing field is implemented by inducing a tilt to the $J_0 \cos(\phi)$ potential

$$H(t) = \phi J_0 \delta I \cos(\omega_p t) \quad (24)$$

ω_p : Probing frequency

δI : Relative amplitude ($\delta I = 10^{-3}$)

Quantum equivalent of the second Josephson relation

$$V = \frac{E_C}{e_*} \delta n. \quad (25)$$

Numerical Conductivity

Using Ohm's law in frequency space

$$I(\omega)d = \sigma(\omega)V(\omega). \quad (26)$$

Using the second Josephson relation $V \sim \delta n$, the numerical conductivity is

$$\sigma(\omega_p) = \frac{I_0}{2} \frac{e_* d}{E_c} \frac{1}{\delta n(\omega_p)}, \quad (27)$$

with the discretized Fourier transformation

$$\delta n(\omega_p) = \frac{\Delta t}{T} \sum_{t=t_0}^{t_0+T} \langle \delta n \mathcal{V}(t_0, t) \rho_S(t_0) \rangle e^{i\omega t}. \quad (28)$$

Analytical conductivity in the London picture

In the limit $\sin \approx \phi$, the imaginary conductivity of the junction, in a probing field, is

$$\sigma_2 = \frac{2\pi}{\Phi_0} \frac{\hbar e_* d}{E_c} \left(\frac{\omega_{\text{Jp}}^2}{\omega} - 1 \right) \quad (29)$$

Analytical conductivity in the London picture

In the limit $\sin \approx \phi$, the imaginary conductivity of the junction, in a probing field, is

$$\sigma_2 = \frac{2\pi}{\Phi_0} \frac{\hbar e_* d}{E_c} \left(\frac{\omega_{\text{Jp}}^2}{\omega} - 1 \right) \quad (29)$$

thus, as $\omega \rightarrow 0$, the London picture response is obtained

$$\sigma_2(\omega) = \frac{2\pi}{\Phi_0} \frac{J_0 e_* d}{\hbar \omega}. \quad (30)$$

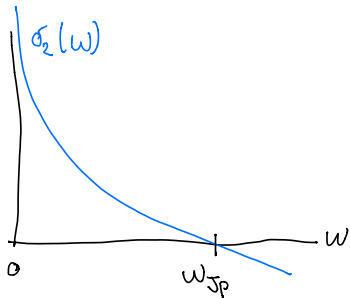
Analytical conductivity in the London picture

In the limit $\sin \approx \phi$, the imaginary conductivity of the junction, in a probing field, is

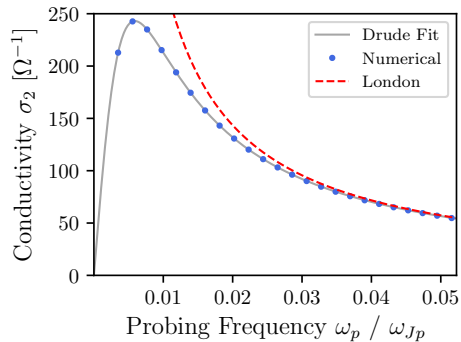
$$\sigma_2 = \frac{2\pi}{\Phi_0} \frac{\hbar e_* d}{E_c} \left(\frac{\omega_{\text{Jp}}^2}{\omega} - 1 \right) \quad (29)$$

thus, as $\omega \rightarrow 0$, the London picture response is obtained

$$\sigma_2(\omega) = \frac{2\pi}{\Phi_0} \frac{J_0 e_* d}{\hbar \omega}. \quad (30)$$



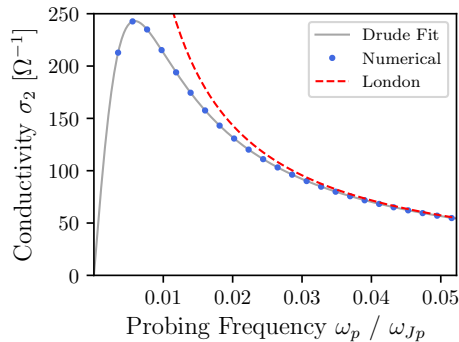
Equilibrium junction in a probing field



Drude response

$$\sigma_2(\omega) \sim J_{\text{eff}} \frac{\gamma_s \omega}{\gamma_s^2 + \omega^2} \quad (31)$$

Equilibrium junction in a probing field



Drude response

$$\sigma_2(\omega) \sim J_{\text{eff}} \frac{\gamma_s \omega}{\gamma_s^2 + \omega^2} \quad (31)$$

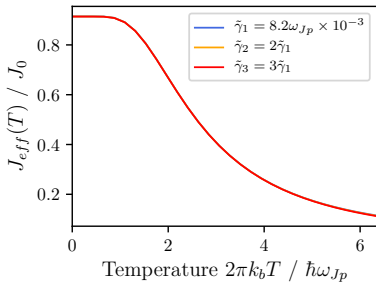
Plasma frequency $\omega_{Jp} = \sqrt{E_c J_{\text{eff}}}$ equals zero-crossing $\sigma_2(\omega_{Jp})$.

Response at $T > 0$

Drude response

$$\sigma_2(\omega) \sim J_{\text{eff}} \frac{\gamma_s \omega}{\gamma_s^2 + \omega^2} \quad (32)$$

From fitting the Drude-form in the relaxation regime, an effective Josephson energy $J_{\text{eff}}(T)$ can be synthesized.



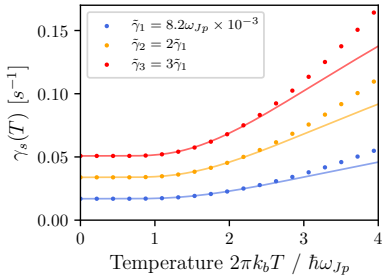
Response at $T > 0$

Drude response

$$\sigma_2(\omega) \sim J_{\text{eff}} \frac{\gamma_s \omega}{\gamma_s^2 + \omega^2} \quad (33)$$

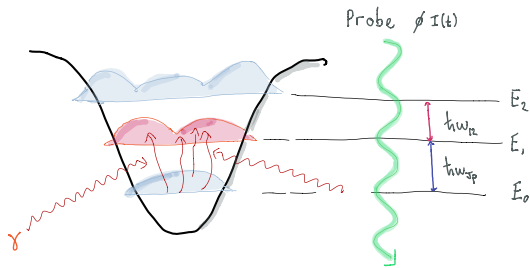
Contrary, the relaxation energy $\hbar\gamma_s(T)$ grows in terms of the Boltzmann factor of the plasma energy $\hbar\omega_{Jp}$.

$$\gamma_s(T) = \gamma_s(0) \left(1 + \exp \left(\frac{\hbar\omega_{Jp}}{k_b T} \right) \right) \quad (34)$$



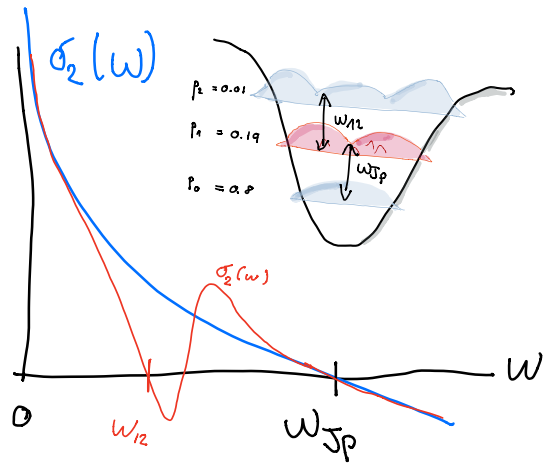
Thermal response

For temperatures above $2\pi k_b T / \hbar\omega_{Jp} \gtrsim 1$, excited states of the system become occupied.



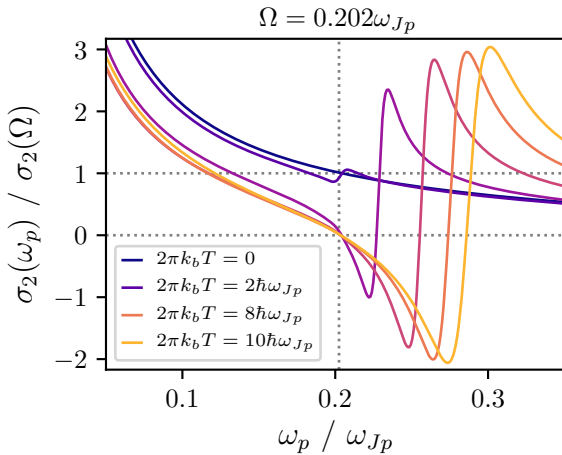
Thermal modes

Additional zero-crossings, at thermally activated transition frequencies, emerge: *Thermal modes*.



Thermal modes

At high temperatures, additional zero-crossings $\sigma_2(\Omega) = 0$ appear in the superconductive response for a probing frequency equal to a transition frequency Ω between excited states.



Dynamical Control

Pump-Probe

Parametric driving of a bilayer system of Josephson junctions lead to an enhancement of the low-frequency conductivity[OCM16, OHCM17].

The Josephson energy is modulated by the following driving Hamiltonian

$$H_d(t) = J_0 A \cos(\omega_d t) \cos \phi, \quad (35)$$

Analytical response

In the limit of small phase $\sin \phi \approx \phi$, going into frequency space by Fourier transforming the equation of motion, one obtains a set of linear equations corresponding to the harmonics of $\cos(\omega_d t)$, which is solved by matrix inversion[OCM16]. Truncating higher harmonic contributions ($m = 1$) and solving a set of three linear equations gives the conductivity

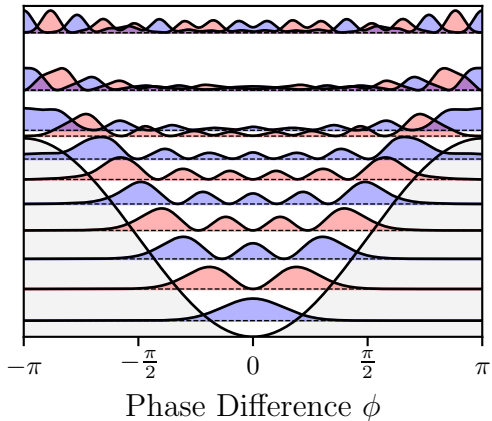
$$\sigma(\omega_p) = \frac{2\pi}{\Phi_0} \frac{\hbar e_* d}{iE_c \omega_p} \left[\frac{A^2 \omega_{Jp}}{4} (C_+(\omega_p) + C_-(\omega_p)) + \omega_p^2 + i\gamma\omega_p - \omega_{Jp}^2 \right], \quad (36)$$

where $C_{\pm}(\omega_p) = (\omega_{Jp}^2 - (\omega_d \pm \omega_p)(\mp i\gamma + \omega_d \pm \omega_p))^{-1}$.

pump-probe in the Josephson regime

Consider a junction in the Josephson regime

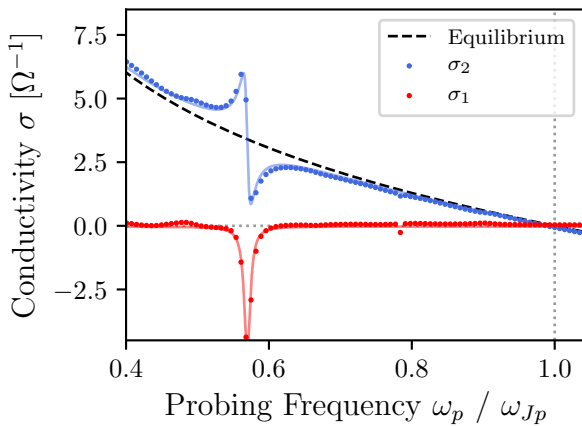
$$\eta = \frac{E_c}{J_0} = \frac{1}{9} \quad (37)$$



pump-probe experiment in the Josephson regime

Driving the junction at a blue-detuned ($\omega_d = \omega_{Jp} + \delta$) frequency leads to an enhancement of σ_2 for probing frequencies below the pole

$$\omega_p < \omega_* \equiv \omega_d - \omega_{Jp} \sim 0.58\omega_{Jp} \quad (38)$$



Conclusions

Response $\sigma_2(\omega_p)$ in good agreement to studies by Okamoto et al. [OCM16, OHCM17, Hom18].

Conclusions

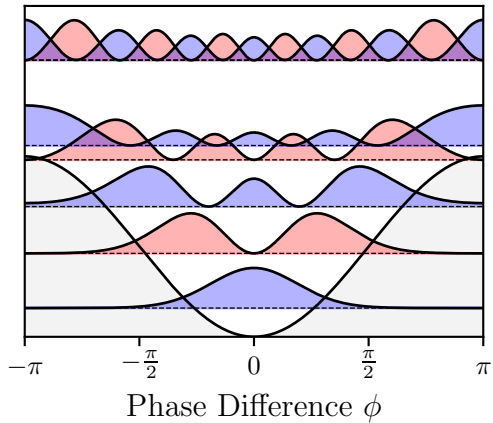
Response $\sigma_2(\omega_p)$ in good agreement to studies by Okamoto et al. [OCM16, OHCM17, Hom18].

The analytical model allows to read out the system parameters by functional fit.

pump-probe experiment in the charge regime

Consider a junction near the charge regime

$$\eta = \frac{E_c}{J_0} = \frac{2}{4.5} \quad (39)$$



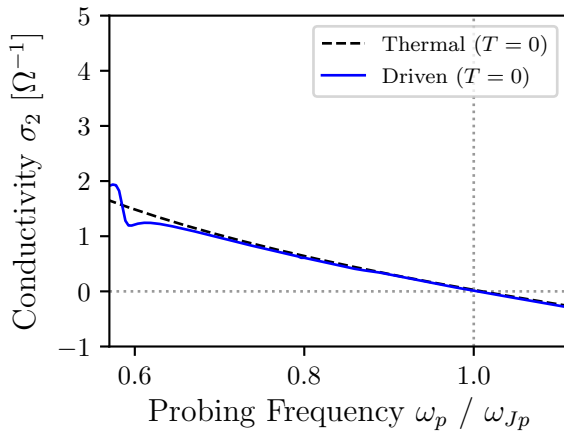
pump-probe experiment in the charge regime

Consider a blue-detuned driving frequency of $\omega_d \approx 1.6\omega_{J_p}$.

pump-probe experiment in the charge regime

Consider a blue-detuned driving frequency of $\omega_d \approx 1.6\omega_{Jp}$.

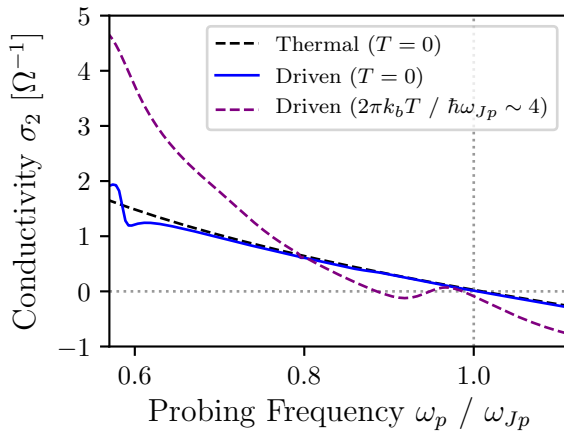
Parametrically induced pole at $\omega_* \sim 0.6\omega_{Jp}$.



pump-probe experiment in the charge regime

Consider a blue-detuned driving frequency of $\omega_d \approx 1.6\omega_{Jp}$.

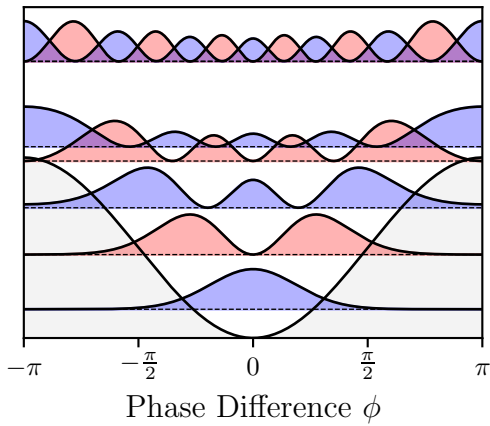
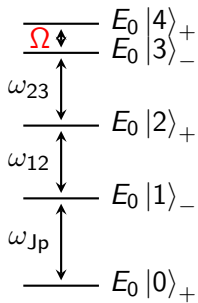
Parametrically induced pole at $\omega_* \sim 0.6\omega_{Jp}$.



Spectrum of the system

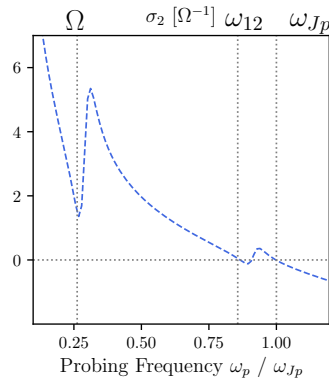
Identify transition frequencies which are in the low probing spectrum ($\omega_p < \omega_{Jp}$).

$$\eta = \frac{2}{4.5} \quad (40)$$



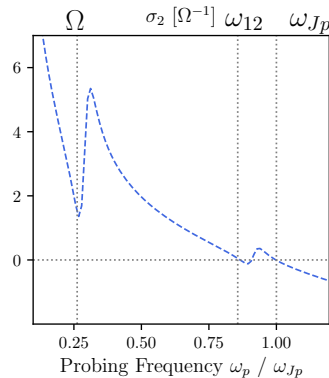
Equilibrium response at high temperatures

At high temperatures $2\pi k_b T / \hbar\omega_{Jp} = 4.75$, thermal modes emerge at the transition frequencies Ω , ω_{12}



Equilibrium response at high temperatures

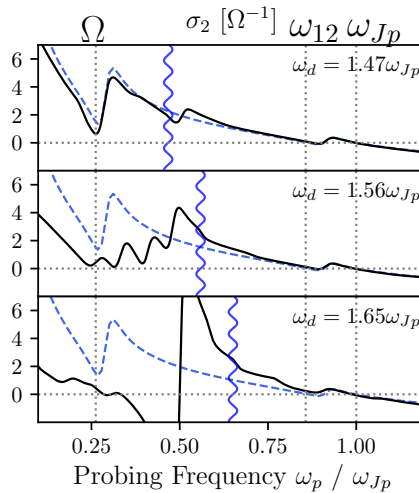
At high temperatures $2\pi k_b T / \hbar\omega_{Jp} = 4.75$, thermal modes emerge at the transition frequencies Ω , ω_{12}



Thermal modes couple to the pump pulse.

Thermal modes + parametric driving

Thermal modes couple to the pump pulse



The pole $\omega_* = \omega_d - \omega_{Jp}$ is depicted as blue wiggled vertical line.

Conclusion

- ▶ At $T = 0$ the response in a steady state pump-probe experiment, of a junction in the Josephson regime $\eta = 0.11$, matches with analytical expectation.
- ▶ Thermal modes couple to the pump pulse.

London picture definitions

Recall that the superconductive response is

$$\sigma_2(\omega) = \frac{2\pi}{\Phi_0} \frac{J_0 e_* d}{\hbar\omega}, \quad (41)$$

as $\omega \rightarrow 0$.

London picture definitions

Recall that the superconductive response is

$$\sigma_2(\omega) = \frac{2\pi}{\Phi_0} \frac{J_0 e_* d}{\hbar\omega}, \quad (41)$$

as $\omega \rightarrow 0$.

This motivates a definition of an effective Josephson energy

$$J_{\text{eff}} \sim \lim_{\omega \rightarrow \infty} \text{Im} \omega \sigma(\omega), \quad (42)$$

London picture definitions

Recall that the superconductive response is

$$\sigma_2(\omega) = \frac{2\pi}{\Phi_0} \frac{J_0 e_* d}{\hbar\omega}, \quad (41)$$

as $\omega \rightarrow 0$.

This motivates a definition of an effective Josephson energy

$$J_{\text{eff}} \sim \lim_{\omega \rightarrow \infty} \text{Im} \omega \sigma(\omega), \quad (42)$$

which evaluates to

$$J_{\text{eff}} = J_0 \left[1 - \frac{A^2 \omega_{\text{Jp}}^2 (\omega_{\text{Jp}}^2 - \omega_d^2)}{2(\omega_{\text{Jp}}^2 - \omega_d^2)^2 + 2\gamma^2 \omega_d^2} \right]. \quad (43)$$

Numerical effective Josephson energy

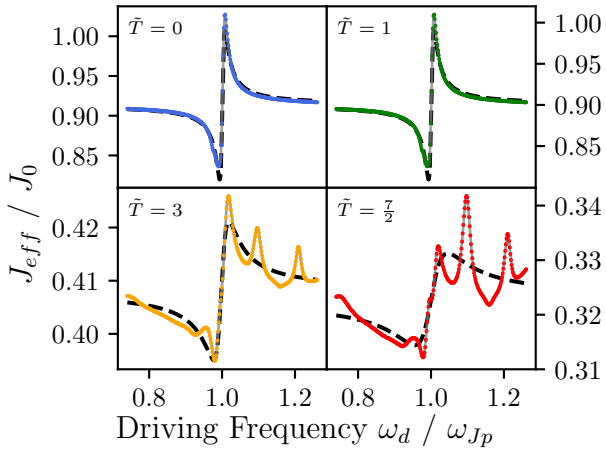
Recall, the Drude-form

$$\sigma_2(\omega) \sim J_{\text{eff}} \frac{\gamma_s \omega}{\gamma_s^2 + \omega^2} \quad (44)$$

is fitted against the numerical σ_2 in order to extract the effective Josephson energy.

Numerical result compared to the analytical model

The pump-probe experiments are set up for a junction in the Josephson regime, at different temperatures $\tilde{T} = 2\pi k_b T / \hbar\omega_{Jp}$.



Numerical result compared to the analytical model

From $J_{\text{eff}}(\omega_d)$ at $T = 0$, the correct simulation parameters are determined by functional fit.

Numerical result compared to the analytical model

From $J_{\text{eff}}(\omega_d)$ at $T = 0$, the correct simulation parameters are determined by functional fit.

Fano-Feshbach resonance is transparent to thermal fluctuations
 $2\pi k_b T / \hbar\omega_{\text{Jp}} < 1$.

Numerical result compared to the analytical model

From $J_{\text{eff}}(\omega_d)$ at $T = 0$, the correct simulation parameters are determined by functional fit.

Fano-Feshbach resonance is transparent to thermal fluctuations
 $2\pi k_b T / \hbar\omega_{\text{Jp}} < 1$.

The classical damping rate grows with temperature.

Numerical result compared to the analytical model

From $J_{\text{eff}}(\omega_d)$ at $T = 0$, the correct simulation parameters are determined by functional fit.

Fano-Feshbach resonance is transparent to thermal fluctuations
 $2\pi k_b T / \hbar\omega_{\text{Jp}} < 1$.

The classical damping rate grows with temperature.

At high temperatures, thermal features in $J_{\text{eff}}(\omega_d)$ emerge.

Numerical result compared to the analytical model

From $J_{\text{eff}}(\omega_d)$ at $T = 0$, the correct simulation parameters are determined by functional fit.

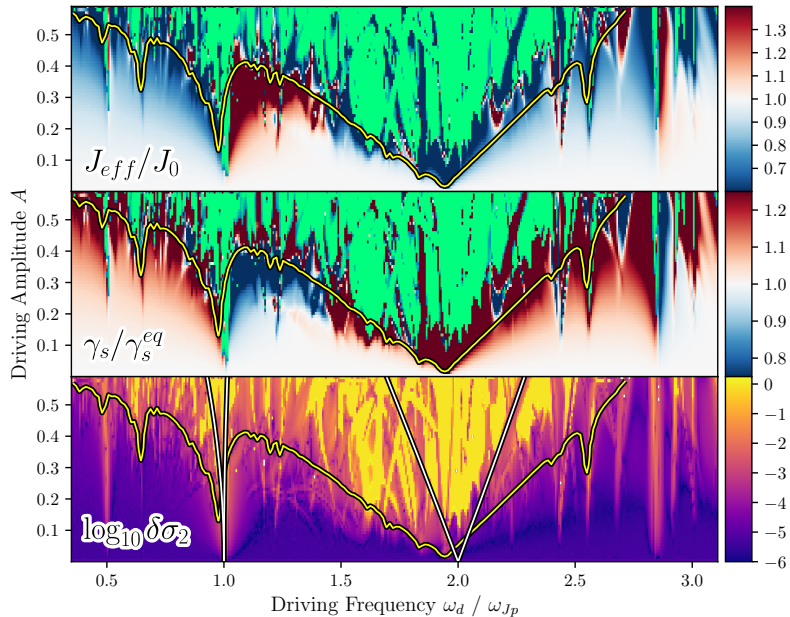
Fano-Feshbach resonance is transparent to thermal fluctuations
 $2\pi k_b T / \hbar\omega_{\text{Jp}} < 1$.

The classical damping rate grows with temperature.

At high temperatures, thermal features in $J_{\text{eff}}(\omega_d)$ emerge.

We could not identify the peaks with energy scales of the system.

Driving far from the plasma resonance



Driving far from the plasma resonance

The effective Josephson energy J_{eff} behaves contrary to the relaxation energy $\hbar\gamma_s$

Increase of current fluctuations corresponds to unstable relaxation regimes

Sub-Fano-Feshbach resonance at $\omega_d \approx 3\omega_{\text{Jp}}$.

Summary

Quantum Josephson junction coupled thru dipole interaction to the electric field.

Quantum Josephson junction coupled thru dipole interaction to the electric field.

An optimized solver for weak coupling master equation forms the base for all numerical experiments.

Quantum Josephson junction coupled thru dipole interaction to the electric field.

An optimized solver for weak coupling master equation forms the base for all numerical experiments.

Due to the discrete energy spectrum, certain energy scales become available at high thermal states.

Quantum Josephson junction coupled thru dipole interaction to the electric field.

An optimized solver for weak coupling master equation forms the base for all numerical experiments.

Due to the discrete energy spectrum, certain energy scales become available at high thermal states.

Thermal modes can be controlled dynamically as they couple to the pump pulse.

Quantum Josephson junction coupled thru dipole interaction to the electric field.

An optimized solver for weak coupling master equation forms the base for all numerical experiments.

Due to the discrete energy spectrum, certain energy scales become available at high thermal states.

Thermal modes can be controlled dynamically as they couple to the pump pulse.

An effective Josephson energy, analogue to the London picture definition, was read from the relaxation regime.

Thank you!

- [AR63] P. W. Anderson and J. M. Rowell. Probable observation of the josephson superconducting tunneling effect. *Phys. Rev. Lett.*, 10:230–232, Mar 1963.
- [BP02] Heinz-Peter Breuer and Francesco Petruccione. *The theory of open quantum systems*. Oxford University Press Inc., New York, 2002.
- [Hom18] Guido F. Homann. Optically Enhanced Interlayer Tunneling in High-Temperature Superconductors. Master's thesis, University of Hamburg, Nov 2018.
- [HZR⁺15] R. Höppner, B. Zhu, T. Rexin, A. Cavalleri, and L. Mathey. Redistribution of phase fluctuations in a periodically driven cuprate superconductor. *Physical Review B*, 91(10):104507, Mar 2015.
- [Jos62] B.D. Josephson. Possible new effects in superconductive tunnelling. *Physics Letters*, 1(7):251 – 253, 1962.
- [LLL35] F. London, H. London, and Frederick Alexander Lindemann. The electromagnetic equations of the

supraconductor. *Proceedings of the Royal Society of London. Series A - Mathematical and Physical Sciences*, 149(866):71–88, 1935.

- [OCM16] Jun-ichi Okamoto, Andrea Cavalleri, and Ludwig Mathey. Theory of Enhanced Interlayer Tunneling in Optically Driven High- T_c Superconductors. *Physical Review Letters*, 117:227001, Nov 2016.
- [OHC17] Jun-ichi Okamoto, Wanzheng Hu, Andrea Cavalleri, and Ludwig Mathey. Transiently enhanced interlayer tunneling in optically driven high- T_c superconductors. *Physical Review B*, 96:144505, Oct 2017.